Emergence of Cooperativity in Plasticity of Soft Glassy Materials

Antoine Le Bouil, Axelle Amon, Sean McNamara, and Jérôme Crassous
Université de Rennes 1, Institut de Physique de Rennes (UMR UR1-CNRS 6251), Bât. 11A, Campus de Beaulieu, F-35042 Rennes, France

(Received 23 July 2013; revised manuscript received 28 February 2014; published 18 June 2014)

The elastic coupling between plastic events is generally invoked to interpret plastic properties and the failure of amorphous soft glassy materials. We report an experiment where the emergence of a self-organized plastic flow is observed well before the failure. For this we impose an homogeneous stress on a granular material, and measure local deformations for very small strain increments using a light scattering setup. We observe a nonhomogeneous strain that appears as transient bands of mesoscopic size and a well-defined orientation, which is different from the angle of the macroscopic frictional shear band that appears at the failure. The presence and the orientation of those microbands may be understood by considering how localized plastic reorganizations redistribute stresses in a surrounding continuous elastic medium. We characterize the length scale and persistence of the structure. The presence of plastic events and the mesostructure of the plastic flow are compared to numerical simulations.

DOI: 10.1103/PhysRevLett.112.246001 PACS numbers: 83.50.-v, 62.20.F-, 62.20.M-, 83.80.Fg

Amorphous materials have intermediate mechanical properties between solids and liquids. At low stress, they behave as elastic solids, but deform plastically and flow when the stress increases. These generic behaviors, observed in many different systems such as concentrated emulsions [1], colloidal systems [2], foams [3] or molecular glasses [4] with apparently universal plastic or rheological laws [5,6], suggest that such materials may be described using a common framework [1,7,8]. At the center of those descriptions is the hypothesis of localized reorganizations. Such events have been observed in many different studies [3,4,9,10]. Each event modifies locally the mechanical equilibrium, causing the surrounding material to deform, and creating internal stresses. These stresses may then provoke other events, leading to a succession or avalanche of events [11,12]. The coupling between events, and its relevance to an avalanchelike cascade scenario for the description of the final persistent shear band is still an open question [12,13].

Several experimental works show isolated reorganizations followed by localized flow structures, suggesting the existence of such coupling. Conclusions remain elusive in direct observation of colloidal glasses due to the dominance of thermal activity over the triggered events [9]. In athermal systems such as granular materials [10] or foams [3], the steps between the accumulation of individual events and the appearance of shear bands remain unclear. Very recent numerical and theoretical results suggest that reorganization events may indeed couple in order to produce bands [12,14–18]. However, the bands observed numerically resulting from the interacting local events are transient and correspond to self-healing microcracks, of a different nature than the final persistent shear bands. To our knowledge such transient microbands forming a clear intermittent structure have never been reported experimentally.

We present in this Letter the first direct experimental evidence showing the progressive emergence of cooperative effects during plastic deformations of an amorphous material. For this, we use a very sensitive light scattering setup to monitor the homogeneous biaxial compression of a granular material. We then show that the plastic flow at the early stage of the loading of a granular material is concentrated along self-healing microbands. The orientation of those transient microbands are clearly different from the Mohr-Coulomb angle of the final permanent shear band. We show that the orientations of those microbands are given by the Eshelby solution [19] for the long-range stress redistribution induced by local plastic reorganizations in an elastic material. We also show that the transient microbands are more prominent as the rupture is approached.

Experimental setup.—We deform an assembly of glass spheres by imposing a homogeneous stress with a biaxial apparatus. We recall here the main features of the setup described extensively elsewhere [20]: The material (glass beads, diameter $d = 90 \pm 20$ μm, volume fraction ≈ 0.60) is placed between a preformed latex membrane (size $85 \times 55 \times 25$ mm) and a glass plate. A pump produces a partial vacuum inside the membrane, creating a confining stress $-\sigma_{xx}$. The confined sample is positioned on a metallic structure [in light gray on Fig. 1(a)]. The glass plate is not represented on Fig. 1(a) and is at the front. The back metallic plate and the front glass plate forbid displacement normal to the x-y plane, ensuring plane-strain conditions. The bottom of the sample rests on a fixed plate, while the upper plate (dark gray) is displaced by a step motor. The stress on the moving plate is $-\sigma_{yy} = -\sigma_{xx} + F/S$, where F is the force measured by a sensor fixed to the plate, and S is the section of the sample. Although there is probably some

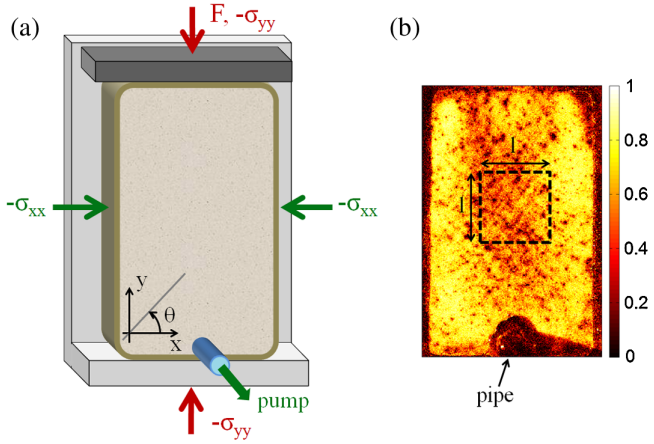

FIG. 1 (color online). (a) Schematic representation of the biaxial setup. The granular material is enclosed between a latex membrane and a glass plate (not represented here). A partial vacuum inside the membrane creates a confining stress $-\sigma_{xx}$. The sample is compressed at a fixed velocity along the y axis through a moving plate (upper plate, dark gray). The light gray back plate as well as the glass plate at the front forbid displacements along the z direction ensuring plane-strain conditions. For compression, $-\sigma_{xx}, -\sigma_{yy} > 0$. (b) A map of correlation $g_I(\epsilon, \mathbf{r})$ with a color scale. The dashed area of side $l \simeq 270d$ is the region of interest for the spatial correlation calculation.

solid friction between the granular material and the plates, we do not observe noticeable differences of deformation between the upper and lower part of the sample. The stress gradient due to gravity is negligible, and the value of confining stress is such that cohesion effects and the crushing of particles are unimportant. The global macroscopic deformation is calculated as $\epsilon = -\epsilon_{yy} = \delta/L$ with δ the upper plate displacement and L the sample height [see left inset of Fig. 2(a)]. The compressions are done at fixed deformation rate $d\epsilon/dt = 1.1 \times 10^{-5}$ s^{-1}. We checked that we were in the quasistatic limit.

Strain heterogeneities are observed using a dynamic light scattering setup [21]. An expanded 532 nm laser beam illuminates the material. Because of the coherence of the light source, interferences occur and a speckle pattern forms. The image of the front side of the sample is recorded by a 7360 × 4912 camera. Two different speckle images are compared using a correlation method explained elsewhere [21]. Images are subdivided in square zones, and for each zone we calculate the normalized correlation function

$$g_I^{(1,2)} = \frac{\langle I_1 I_2 \rangle - \langle I_1 \rangle \langle I_2 \rangle}{\sqrt{\langle I_1^2 \rangle - \langle I_1 \rangle^2}\sqrt{\langle I_2^2 \rangle - \langle I_2 \rangle^2}}, \qquad (1)$$

where I_1 and I_2 are the intensity matrices of a same zone in two different images, and $\langle \cdots \rangle$ indicates the average over the zone. Each zone becomes a pixel in a correlation map [see Fig. 1(b) and the movie in the Supplemental Material [22]], corresponding to a volume of surface $\sim 2.1d \times 2.1d$ in the x-y plane and of depth of few d. The decorrelation of the scattered light comes from relative bead motions. We thus measure a combination of affine and nonaffine bead displacements, and the rotation of nonspherical beads. In the following, we present maps based on images made at sample deformations ϵ and $\epsilon + 3.2 \times 10^{-5}$, and we note $g_I(\epsilon, \mathbf{r})$ the value of the normalized correlation at compression ϵ and at position $\mathbf{r}$ [see Fig. 1(b)].

Plastic flow structure.—Figure 2(a) shows the evolution of the stress difference $\sigma_{xx} - \sigma_{yy}$ as a function of the deformation ϵ. At the beginning of the loading, $\sigma_{xx} - \sigma_{yy}$ increases with ϵ, and then attains a plateau, consistent with numerous preceding studies, where a granular material was prepared near the critical state volume fraction [23]. The stress plateau at $\epsilon_c = 4.66\%$ corresponds to the failure of the sample, confirmed by the correlation map shown in Fig. 2(a) (rightmost inset). The deformation is dominated by two symmetric shear bands where $g_I(\epsilon, \mathbf{r})$ is low, corresponding to highly localized deformation. The inclination of the bands is $\theta \simeq 65°$, in agreement with a Mohr-Coulomb analysis $\theta_{MC} = 45 + \varphi_c/2 \simeq 63°$ for a frictional material, with φ_c the internal friction angle [24]. $\varphi_c = \arcsin[(\sigma_{yy} - \sigma_{xx})/(\sigma_{yy} + \sigma_{xx})]$ at failure ($\epsilon = \epsilon_c$). Those bands are permanent in the sense that they do not evolve with ϵ once they appear (see the movie in the Supplemental Material [22]).

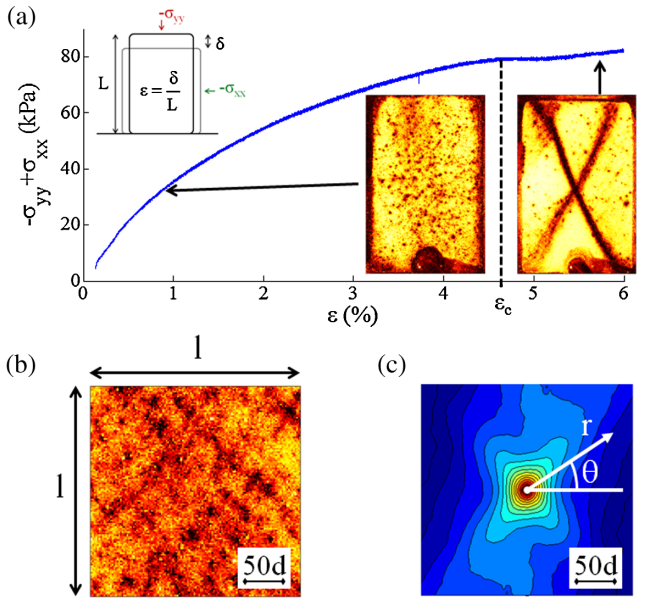

FIG. 2 (color online). (a) Applied stresses difference versus deformation ($-\sigma_{xx} = 30$ kPa). Insets: Left, notations; right: maps of $g_I(\epsilon, \mathbf{r})$ before failure ($\epsilon = -\epsilon_{yy} = 0.91\%$) and after failure ($\epsilon = 5.82\%$). (b) Enlargement of the region of interest of the deformation map before failure ($\epsilon = 3.30\%$) showing the mesoscale strain heterogeneities. (c) Correlation function $\Psi^{(0)}(\epsilon, \mathbf{r})$ of g_I at $\epsilon = 3.30\%$ showing the plastic flow structure in a square of size $l \simeq 270d$ in the $\mathbf{r}$ plane.

Figure 2(b) shows a map of deformation before failure. The deformation is strongly heterogeneous with a complicated fine structure at small scale. In contrast with the permanent shear bands observed after failure, this deformation pattern fluctuates strongly during the loading (see the movie in the Supplemental Material [22]). To investigate the spatial structure and intermittency of the plastic flow, we consider the spatial correlation function of $g_I' \equiv 1 - g_I$:

$$\Psi^{(\Delta\epsilon)}(\epsilon, \mathbf{r}) = \langle g_I'(\epsilon + \Delta\epsilon/2, \mathbf{r}') g_I'(\epsilon - \Delta\epsilon/2, \mathbf{r} + \mathbf{r}') \rangle - \langle g_I'(\epsilon + \Delta\epsilon/2, \mathbf{r}') \rangle \langle g_I'(\epsilon - \Delta\epsilon/2, \mathbf{r} + \mathbf{r}') \rangle, \quad (2)$$

where $\langle \cdots \rangle$ is an average over 100 correlation maps, i.e., a deformation of 3.2×10^{-3}, and over $\mathbf{r}'$, for $\mathbf{r}'$ and $\mathbf{r} + \mathbf{r}'$ covering the region of interest on Fig. 1(b). Figure 2(c) shows a plot of $\Psi^{(0)}(\epsilon, \mathbf{r})$. Along two symmetric directions $\theta = \pm\theta_E$ with $\theta_E \approx 53°$ the correlation decays slowly with r [see Fig. 4(a)]. The direction of the anisotropy θ_E is almost constant during the loading, and is clearly different from θ_{MC}.

Localized plastic events.—To explain the observed structure of the plastic flow we first investigate theoretically the consequences of a single, isolated reorganization somewhere in the granular material. Consider a plastic deformation that relaxes stress within a small volume, but redistributes it in the surrounding material. We consider that the surrounding region behaves as a linear elastic material [25], that we will suppose isotropic with Poisson ratio ν. Eshelby gave an analytical solution to this 3D problem [19]: Let $\mathbf{e}^*$ be the strain tensor of the reorganization [see Fig. 3(a)]. We suppose $e^*_{xy} = 0$, i.e., that $\mathbf{e}^*$ is coaxial to the applied stress tensor and $e^*_{zz} = e^*_{xz} = e^*_{yz} = 0$ because of the plane-strain configuration, leaving only e^*_{xx} and e^*_{yy} as the nonzero strain components. Far from the rearrangement, the additional stress originating from the rearrangement in the x-y plane is $\tilde{\boldsymbol{\sigma}}$, with $\tilde{\sigma}_{xx} - \tilde{\sigma}_{yy} \propto f(\theta)$, where

$$f(\theta) = (e^*_{xx} - e^*_{yy}) \left[-\frac{15}{4} \cos(4\theta) + \frac{8\nu - 7}{4} \right] - \frac{9}{2} (e^*_{xx} + e^*_{yy}) \cos(2\theta). \quad (3)$$

If $\tilde{\sigma}_{xx} - \tilde{\sigma}_{yy} > 0$ the redistributed stress adds to the applied stress, increasing strain along those directions. Its maximum occurs for $\cos(2\theta^*_E) = (3/10)(e^*_{yy} + e^*_{xx})/(e^*_{yy} - e^*_{xx})$. In the case of an isovolumic transformation, $\theta^*_E = 45°$ (mod 90°). Figure 3(b) shows $f(\theta)$ in this case. For a local rearrangement in agreement with the macroscopic deformation of the sample, i.e., e^*_{xx} and e^*_{yy} of opposite signs, θ^*_E increases (respectively, decreases) for a dilating (respectively, contracting) rearrangement, with extremal values $\frac{1}{2}\cos^{-1}(\pm 3/10)$. The largest possible value for θ^*_E is then 54°, which is close to the value of $\theta_E \approx 53°$ of the experiment. This reorganization structure has been shown in numerical studies of molecular glasses [12,14] and cellular foam [3], but the existence of such an elastic redistribution in frictional granular material is still an open question. Indeed, the existence of an elastic limit for such a system is still a matter of debate [25]. We performed numerical bidimensional discrete element method simulations of a biaxial compression test [see Fig. 3(c) for boundary conditions]. Figure 3(d) shows results from a simulation of $N = 256^2$ grains, using a visualization method inspired by the experimental technique: Positions of the grains are recorded at strain increments of $\delta\epsilon = 10^{-5}$. Two successive system states are compared, and for each grain, a local strain (average relative change in distance to its neighbors) is calculated. Those grains whose local strain is large are dark. We can generate a plastic event in the simulation by softening a small number of grains in the sample [see Fig. 3(e)] and we obtain a local deformation in accordance with the analytical solution of Fig. 3(b). Figure 3(d) shows that such local events also occur during the compression of the granular material.

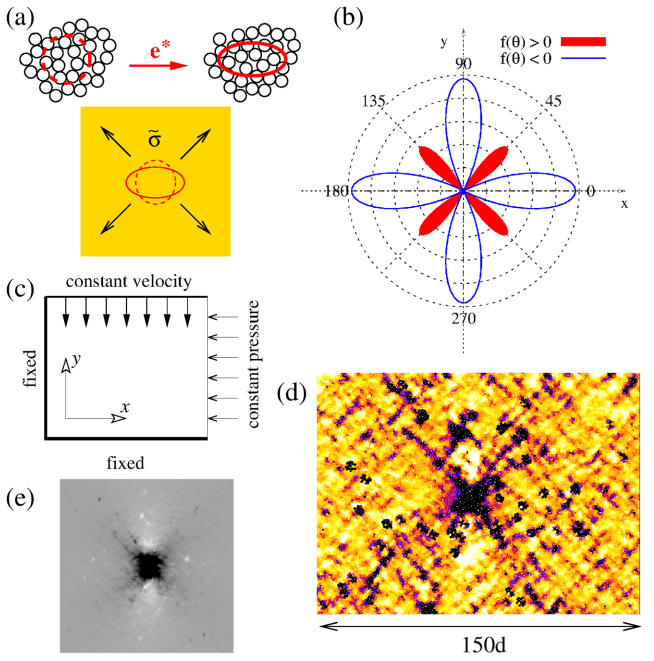

FIG. 3 (color online). (a) Schematic representation of a local plastic event specifying the tensors $\mathbf{e}^*$ (linked to the deformation of the inclusion) and $\tilde{\boldsymbol{\sigma}}$ (stress redistribution in the surrounding medium due to the plastic event). (b) Angular distribution of $\tilde{\sigma}_{xx} - \tilde{\sigma}_{yy} \propto f(\theta)$ in the case of an isovolumic transformation of the inclusion ($\nu = 0.33$). (c) Boundary conditions of the numerical simulations. (d) Example of a deformation map from numerical simulation displaying a local event and microbands. (e) Synthetic local reorganization obtained numerically by a modification of the elastic constants of few grains.

Coupling between localized events and plastic flow structure.—Along the directions where $\tilde{\sigma}_{xx} - \tilde{\sigma}_{yy}$ is positive, the additional stress has the same sign as the applied stress, possibly triggering new reorganizations. We therefore expect deformation to be organized in microbands whose orientations are given by the Eshelby solution. This structure is visible in the numerical experiments where very transient localized lines inclined at $\theta \approx \pm 45°$ are present [see Fig. 3(d)]. The resulting images display the same phenomenology as the experimental results: Well before failure, deformation is concentrated in short diagonal microbands (probably similar to those reported in other studies [18,26,27]), and at failure, a shear band appears (not shown here). The agreement between 2D simulation and 3D experiments supports our plane-strain hypothesis.

Spatial and temporal correlations.—Coming back to our experimental data, we focus on the evolution of the anisotropic part of $\Psi^{(\Delta\epsilon)}(\epsilon, r, \theta) = \Psi^{(\Delta\epsilon)}(\epsilon, \mathbf{r})$ during the loading, which we define as

$$\chi^{(\Delta\epsilon)}(\epsilon, r) = \frac{1}{2}[\Psi^{(\Delta\epsilon)}(\epsilon, r, \theta_E) + \Psi^{(\Delta\epsilon)}(\epsilon, r, -\theta_E)] - \Psi^{(\Delta\epsilon)}_{\text{iso}}(\epsilon, r) \quad (4)$$

with $\Psi^{(\Delta\epsilon)}_{\text{iso}}(\epsilon, r) = \frac{1}{2\pi}\int_0^{2\pi} \Psi^{(\Delta\epsilon)}(\epsilon, r, \theta) d\theta$, the isotropic part of $\Psi^{(\Delta\epsilon)}$. Figure 4(b) shows the evolution of $\chi^{(0)}(\epsilon, r)$ in the function of r for different values of ϵ. We observe that the anisotropic part of the correlation function increases as the loading increases. We consider a twofold characterization of $\chi^{(0)}$. First, the integral $A(\epsilon) = \int_{r=0}^{r=\ell'/2} \chi^{(0)}(\epsilon, r) dr$ estimates the strength of the anisotropy. Second, the characteristic distance $\xi(\epsilon)$ at which the correlation is maximum $(\partial\chi^{(0)}/\partial r)(\epsilon, \xi(\epsilon)) = 0$ is computed using a quadratic fit [plain line of Fig. 4(b)] of the experimental curves near the maximum. Figure 4(c) shows that both the integral A and the characteristic length ξ/d of the anisotropy increase as the loading progresses toward rupture. Finally, the transient nature of the observed structure can be shown by considering the scale of deformation at which the plastic flow persists. For this, we considered the evolution of $(\chi^{(\Delta\epsilon)}/\chi^{(0)})(\epsilon, \xi(\epsilon))$ with $\Delta\epsilon$ at a given ϵ. Figure 4(d) shows that close to rupture, for $\epsilon = 4.4\%$ and $\xi(\epsilon = 4.4\%) = 85d$, the deformation persists after a deformation increment $\Delta\epsilon \approx 0.3\%$. On the contrary, further from the failure ($\epsilon = 3.3\%$), the deformation decays over a typical increment of deformation $\Delta\epsilon \approx 0.02\%$.

From the structure of the plastic flow, a characteristic length ξ revealing the cooperativity of the fluctuation of plastic flow emerges. The values of ξ are in quantitative agreement with numerical simulations of the granular material [26] where fluctuations coupled on distance $\sim(10–40)d$ are reported. Theoretically [30] a nonlocal rule for the mean plastic flow is expected to emerge from those fluctuations. Such nonlocal flow rules have been proposed to describe granular plastic flow [31]. Figure 4(c) shows the expected evolution of the cooperativity length [28] proposed in [29] during the loading. The cooperativity length of the mean flow is smaller than ξ. This is probably due to the coarse-graining process described in [30].

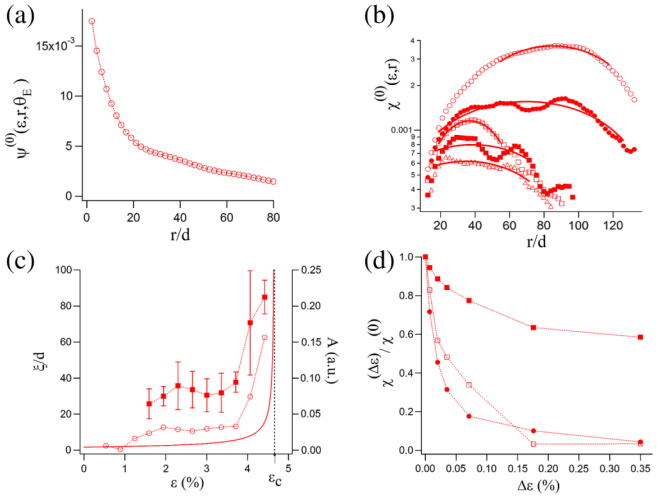

FIG. 4 (color online). (a) $\Psi^{(0)}$ as function of r for $\epsilon = 2.7\%$, showing a fast decay at a short distance ($r/d \lesssim 10$) followed by a slow decay. (b) $\chi^{(0)}(\epsilon, r)$ versus r/d for increasing values of deformations $\epsilon = 1.6\%$ (open triangle), $\epsilon = 2.3\%$ (filled square), $\epsilon = 3.7\%$ (open square), $\epsilon = 4.0\%$ (filled circle), $\epsilon = 4.4\%$ (open circle). Lines are quadratic fits around maximum. (c) Length ξ/d (filled square) and mean amplitude A (open circle) (see text) as functions of the deformation ϵ. Error bars are given by the uncertainty of the quadratic fit of $\chi^{(0)}$ around maximum. The black dotted line indicates the deformation at rupture $\epsilon_c \approx 4.66\%$. The plain line is the cooperative length [28] expected from the nonlocal flow rule of granular material [29]. (d) Relaxation of $(\chi^{(\Delta\epsilon)}/\chi^{(0)})(\epsilon, \xi(\epsilon))$ as a function of the deformation increment $\Delta\epsilon$ for $\xi(\epsilon = 3.3\%) = 33d$ (filled circle), $\xi(\epsilon = 4.0\%) = 70d$ (open square), and $\xi(\epsilon = 4.4\%) = 85d$ (filled square).

Conclusion.—In summary, a careful experimental study of the plastic flow of an athermal amorphous material reveals a mesoscopic structure of the strain since the early stage of the loading process: Deformation concentrates in transient short microbands of well-defined orientation. We connect those orientations with the elastic long-range stress redistribution due to localized plastic reorganizations. We show an increasing characteristic length and persistence during the loading. However, the relationship between these transient microbands and the final permanent frictional shear bands is more complex than the description of a final persistent shear-band formation as a mere growing cascade of local rearrangements. The final shear band does not arise from a coalescence of microbands, nor is it initiated by a single microband that reaches the boundary and becomes locked. Instead, as the movie in the Supplemental Material [22] shows, the two types of deformation, oriented in two different directions, coexist near failure. We observe a hierarchical structure with a mesoscopic pattern embedded in a large scale shear band.

The modelization of the final persistent shear band needs to describe the complex interaction between the microbands and the larger scale localization. The careful characterization of the birth of the permanent shear band is a work in progress.

This work has been supported by ANR (Grant No. 2010-BLAN-0927-01) and Région Bretagne (MideMade). We thank P. Chasle, H. Orain, J.-C. Sangleboeuf, P. Bésuelle and C. Viggiani for help with the biaxial apparatus, and GDR Mephy for fruitful discussions.

[1] J. Goyon, A. Colin, G. Ovarlez, A. Ajdari, and L. Bocquet, Nature (London) **454**, 84 (2008).
[2] R. Besseling, L. Isa, P. Ballesta, G. Petekidis, M. E. Cates, and W. C. K. Poon, Phys. Rev. Lett. **105** 268301 (2010).
[3] A. Kabla, J. Scheibert, and G. Debregeas, J. Fluid Mech. **587**, 45 (2007).
[4] A. Tanguy, F. Leonforte, and J.-L. Barrat, Eur. Phys. J. E **20**, 355 (2006).
[5] P. Sollich, F. Lequeux, P. Hebraud, and M. E. Cates, Phys. Rev. Lett. **78**, 2020 (1997).
[6] C. Derec, A. Ajdari, and F. Lequeux, Eur. Phys. J. E **4**, 355 (2001).
[7] G. Katgert, B. P. Tighe, M. E. Möbius, and M. van Hecke, Europhys. Lett. **90**, 54002 (2010).
[8] V. B. Nguyen, T. Darnige, A. Bruand, and E. Clement, Phys. Rev. Lett. **107**,138303 (2011).
[9] P. Schall, D. A. Weitz, and F. Spaepen, Science **318**, 1895 (2007).
[10] A. Amon, V. B. Nguyen, A. Bruand, J. Crassous, and E. Clément, Phys. Rev. Lett. **108**, 135502 (2012).
[11] M. L. Falk, and J. S. Langer, Phys. Rev. E **57**, 7192 (1998).
[12] C. E. Maloney and A. Lemaître, Phys. Rev. E **74**, 016118 (2006).
[13] K. A. Dahmen, Y. Ben-Zion, and J. T. Uhl, Nat. Phys. **7**, 554 (2011).
[14] M. Tsamados, A. Tanguy, F. Léonforte, and J.-L. Barrat, Eur. Phys. J. E **26**, 283 (2008).
[15] S. M. Talamali *et al.*, C. R. Méc **340**, 275 (2011).
[16] K. Martens, L. Bocquet, and J.-L. Barrat, Soft Matter **8**, 4197 (2012).
[17] R. Dasgupta, H. G. Hentschel, and I. Procaccia, Phys. Rev. Lett. **109** 255502 (2012).
[18] F. Gimbert, D. Amitrano, and J. Weiss, Europhys. Lett. **104**, 46001 (2013).
[19] J. D. Eshelby, Proc. R. Soc. A **241**, 376 (1957).
[20] A. Le Bouil, A. Amon, J.-C. Sangleboeuf, H. Orain, P. Bésuelle, G. Viggiani, P. Chasle, and J. Crassous, Granular Matter **16**, 1 (2014).
[21] M. Erpelding, A. Amon, and J. Crassous, Phys. Rev. E **78**, 046104 (2008).
[22] See Supplemental Material at http://link.aps.org/supplemental/10.1103/PhysRevLett.112.246001 for the successive maps of incremental deformation during the loading shown in Fig. 2(a). The value of the imposed strain is indicated in percent. The color scale is the same as Fig. 1(b).
[23] *Critical State Soil Mechanics*, edited by A. N. Schofield, and C. P. Wroth (McGraw-Hill, New York, 1968)
[24] *Statics and Kinematics of Granular Materials*, edited by R. M. Nedderman (Cambridge University Press, Cambridge, 1992).
[25] H. A. Makse, N. Gand, D. L. Johnson, and L. Schwartz, Phys. Rev. E **70**, 061302 (2004).
[26] M. R. Kuhn, Mech. Mater. **31**, 407 (1999).
[27] S. A. Hall, D. Muir Wood, E. Ibraim, and G. Viggiani, Granular Matter **12** 1 (2010).
[28] The cooperativity length is [29] $\zeta = Ad/\sqrt{\mu_c - \mu}$, with $A = 0.48$. We define here μ from the Mohr-Coulomb analysis: $\mu = \tan(\varphi)$ with $\varphi = \arcsin[(\sigma_{yy} - \sigma_{xx})/(\sigma_{yy} + \sigma_{xx})]$, and μ_c with the value of μ at failure.
[29] D. L. Henann and K. Kamrin, Proc. Natl. Acad. Sci. U.S.A. **110**, 6730 (2013).
[30] L. Bocquet, A. Colin, and A. Ajdari, Phys. Rev. Lett. **103** 036001 (2009).
[31] K. Kamrin, and G. Koval, Phys. Rev. Lett. **108** 178301 (2012).